AD-A148 829 ACTA ELECTRONICA SINICA (SELECTED ARTICLES)(U) FOREIGN TECHNOLOGY DIV WRIGHT-PATTERSON AFB OH Z YOUWEI ET AL. 07 NOV 84 FTD-ID(RS)T-1227-84 1/1

UNCLASSIFIED F/G 12/1 NL

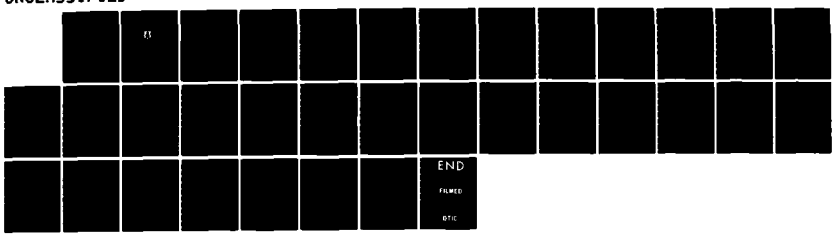

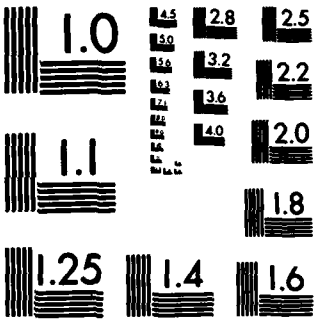

MICROCOPY RESOLUTION TEST CHART
NATIONAL BUREAU OF STANDARDS-1963-A

AD-A148 829

FTD-ID(RS)T-1227-84

FOREIGN TECHNOLOGY DIVISION

ACTA ELECTRONICA SINICA'
(Selected Articles)

DTIC FILE COPY

DEC 1 8 1984

Approved for public release;
distribution unlimited.

84 12 11 021

EDITED TRANSLATION

FTD-ID(RS)T-1227-84 7 November 1984

MICROFICHE NR: FTD-84-C-001068

ACTA ELECTRONICA SINICA
(Selected Articles)

English pages: 29

Source: Dianzi Xuebao, Vol. 11, Nr. 6, November 1983, pp. 47-55; 57-63

Country of origin: China
Translated by: SCITRAN
F33657-81-D-0263
Requester: SDNA
Approved for public release; distribution unlimited.

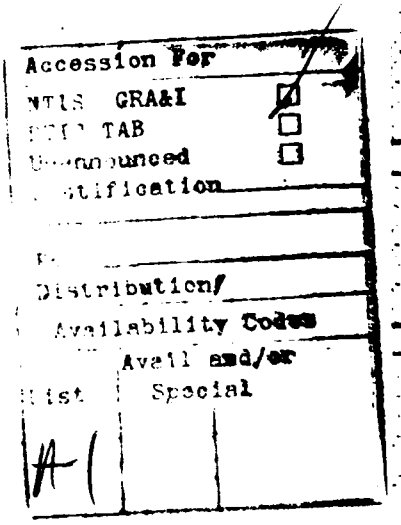

THIS TRANSLATION IS A RENDITION OF THE ORIGINAL FOREIGN TEXT WITHOUT ANY ANALYTICAL OR EDITORIAL COMMENT. STATEMENTS OR THEORIES ADVOCATED OR IMPLIED ARE THOSE OF THE SOURCE AND DO NOT NECESSARILY REFLECT THE POSITION OR OPINION OF THE FOREIGN TECHNOLOGY DIVISION.

PREPARED BY:

TRANSLATION DIVISION
FOREIGN TECHNOLOGY DIVISION
WP-AFB, OHIO.

Table of Contents

GRAPHICS DISCLAIMER

All figures, graphics, tables, equations, etc. merged into this translation were extracted from the best quality copy available.

SIMULATION OF APPLICATION OF KALMAN FILTERING TO AIRBORNE RADAR TRACKING SYSTEM* /47

Zhang Youwei and Zhu Guchuan
(Beijing Institute of Aeronautics and Astronautics)

Abstract: This work introduced the theory and simulation results of employing the Kalman filter in an airborne fire control radar tracking system. It discussed problems such as target dynamics modeling, linear filtering and simulation, linear filtering approximation, sensitivity simulation, maneuvering target tracking and adaptivity. Simulation results showed that the system performed far better than typical systems. Furthermore, its adaptivity to maneuvering targets was better.

Abstract: An application of the Kalman filtering theory and simulation results with computer are developed in tracking system of airborne firecontrol radar. The dynamic mathematical model of target, the linear filtering and simulation, approximation by the linear filtering, sensitivity simulation, maneuvering target tracking and adaptive filtering and etc are showed. Simulating results show that this system is better than general system on the performance and the adaptive capability of maneuvering targets greatly.

I. Introduction

Since the introduction of the Kalman filter, it has primarily been used in tracking and processing of targets in orbits and suborbits or during re-entry. However, very little research on piloted moving targets has been conducted. Since the seventies, a great deal of effort was devoted to the tracking of maneuvering targets. The results, however, are usually limited to specific targets, detectors and environments. Hence, there is a need to find a simple and appropriate model to approach a moving target. The Kalman filter was used to build an advanced tracking system. This work absorbed the valuable portions in References [1-4] and obtained specific results through

*completed in March 1982, revised in March 1983.

theoretical analysis and simulation. It provided a basis for engineering design.

The single pulse (or conical scanning) radar tracking system discussed in this work is shown in Figure 1. The pitch angle error signal E_e, azimuthal angle error signal E_d, range error signal E_r and speed error signal E_v were expressed digitally by the radar receiver and signal processor. The sampling frequency of these data could reach several dozen kHz. The recurrence cycle of a Kalman, however, is usually 10 Hz or slightly higher to satisfy the requirements in closed loop tracking. Therefore, in order to minimize loss of information, a prebalancer was used. To simplify the symbols, the error signals are still denoted as E_e, E_d, E_r and E_v, respectively. The core of the system is the optimum state estimater, where four tracking loops intersect. It could complete Kalman filtering or other forms of iterating filtering. The input quantities include the four error signals E_c, E_d, E_r and E_v, angular velocity components ω_e, ω_d and ω_r of the electric axis of the antenna revolving with respect to the inertia coordinate system, antenna control commands ω_{ce} and ω_{cd}, acceleration components a_e, a_d and a_r of the target in the inertial coordinate system as given by the inertia guidance system, and two directional angles θ_e and θ_d of the antenna coordinate system with respect to the carrier coordinate system. The optimum control command requires the optimum state estimater to output estimated values of angular errors $\hat{E}_e$ and $\hat{E}_d$ as well as angular velocities of the antenna aiming axis $\hat{\omega}_E$ and $\hat{\omega}_D$. In the meantime, estimated values of range error $\hat{R}$ and velocity error $\hat{V}$ are also given. The antenna control command was created by $\omega_{ce}=\hat{\omega}_E+\lambda\hat{\varepsilon}_e$ and $\omega_{cd}=\hat{\omega}_D+\lambda\hat{\varepsilon}_d$. Simulation results showed that λ should be $10 \sim 15$. In addition, $\hat{R}$ and $\hat{V}$ were used to form range gate and velocity gate control commands R_{gc} and V_{gc}, respectively.

The tracking system discussed here is different from classical systems:

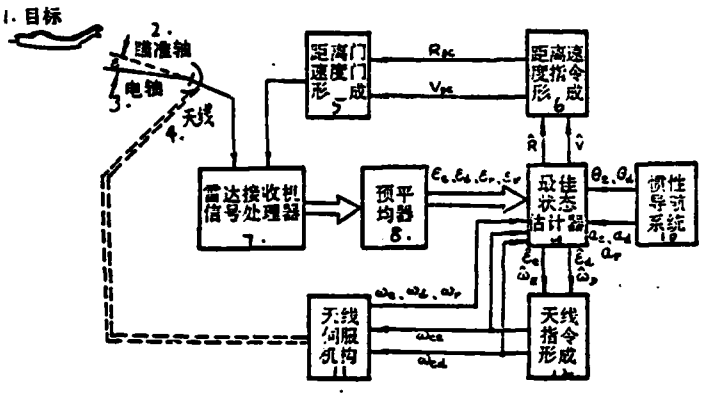

Figure 1. Structure of Tracking System.

Key: 1) target; 2) aiming axis; 3) electric axis; 4) antenna; 5) formation of range gate and velocity gate; 6) formation of range and velocity commands; 7) radar receiver and signal processor; 8) pre-balancer; 9) optimum state estimater; 10) inertial guidance system; 11) antenna servo mechanism; 12) antenna command formation.

(1) A Kalman filter was used to complete error signal filtering, i.e., to extract the true estimated value of an error signal from noise pollution in order to obtain a more accurate deviation signal for tracking.

(2) The use of a Kalman filter could estimate more useful information such as angular velocities $\hat{\omega}_E$ and $\hat{\omega}_D$ of the aiming axis as well as estimated acceleration components $\hat{a}_E$, $\hat{a}_D$ and $\hat{a}_R$ of the target along the aiming axis coordinate system. These could form a quasi-optimal control pattern.

(3) The use of a Kalman filter in the tracking system could naturally form a hinge for all tracking loops. A tracking loop could extract useful information from other loops to further improve the tracking performance. For example, it was demonstrated in simulation that, when the range and velocity tracking loops intersected, the accuracy in ranging could be improved from the classical 10 m to 2 m (mean square root).

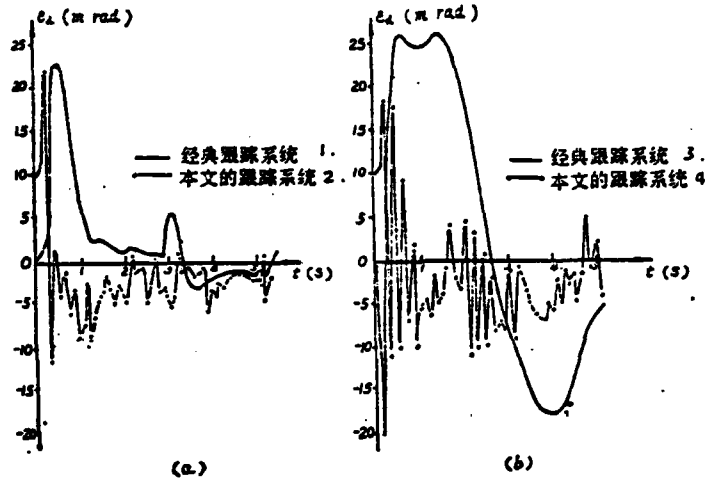

(a) $R_{min} = 4500m$ (b) $R_{min} = 600m$

Figure 2. Comparison of Angular Tracking Error.

Key: 1) classical tracking system; 2) this tracking system; 3) classical tracking system; 4) this tracking system.

(4) The parameters in the filter structure are time dependent. Therefore, the optimal tracking performance may be maintained over a very wide range to allow the system to have a certain adaptivity to target maneuverability.

In order to compare the extent of improvement of the Kalman filtering tracking system relative to a classical system, we also conducted the simulation of a classical angular tracking system under the same conditions. The sampling frequency of the classical simulation system was 10^3 Hz. Results of the /49 simulation are shown in Figure 2.

It showed that the tracking system discussed in this paper had good steady state and transient characteristics. The classical system, however, required a longer transition time. The steady state accuracy could still be maintained for far away targets. For close range moving targets, the tracking performance deteriorated apparently. Thus, the tracking system

discussed in this work is obviously better than classical systems.

II. Target Dynamics Modeling

Model construction is the key to applying Kalman filtering to radar tracking systems. For an airborne tracking system for a single moving target, it involves the inertial coordinate system (N, E, D), carrier coordinate system (X, Y, Z), antenna coordinate system (r, e, d) and aiming axis coordinate system (R, E, D). The first problem is which coordinate system should be used for target dynamics modeling.

The filtering problem in a radar tracking system is actually a non-linear problem. In engineering, it is usually linearized to be followed by an estimation of Kalman filtering. It is a first order approximation. Because the final solution of non-linear filtering has not yet been obtained, there is no rigorous conclusion on the convergence of approximations of various orders. Therefore, we evaluated the characteristics of various coordinate system models through simulation. In order to obtain linear models for both the state and measurement, we also established a differential polynomial dynamic model in the simulation together with three other models mentioned earlier (carrier coordinate system, antenna coordinate system, and aiming axis coordinate system).

The same typical flight pattern was used for the four models during simulation. In the first 4 seconds the relative motion between the target in front and the carrier plane was linear and turning flight. Later, it was close range crossover route flight. Great maneuverability was shown in this case [5]. Figure 3 is a series of simulated curves. Each curve was composed by 110 data points. Results showed that the tracking accuracy is basically the same for tracking systems built by these four models when the mathematical model matches with

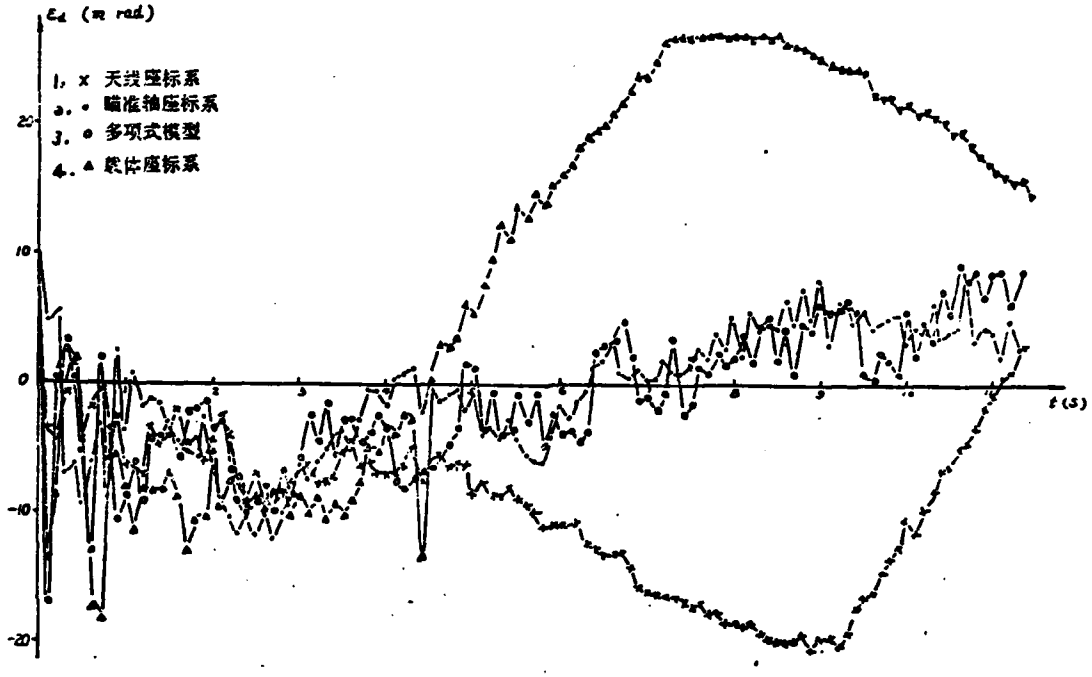

Figure 3. Comparison of Angular Tracking Accuracy of Four Models.

Key: 1) antenna coordinate system; 2) aiming axis coordinate system; 3) polynominal model; 4) carrier coordinate system.

reality. However, under maneuvering conditions, the aiming axis coordinate system and differential polynominal dynamic models are more adaptable than the carrier coordinate system and antenna coordinate system models. Therefore, we used the aiming axis coordinate system in this work.

The aiming axis coordinate system was used in the /50
airborne radar. The first problem encountered was the transformation from an inertial coordinate system through the carrier coordinate system and antenna coordinate system to the aiming axis coordinate system. Next, we should also consider that these four coordinate systems are always in relative motion. It will involve complex dynamic problems. In order to find the equation of state of the radar tracking system, long mathematical

derivations were required. This work could be found in the scientific research reports [6-7] and only the final results are given here. The equation of state of the radar tracking system is:

$$\begin{pmatrix}\dot{\varepsilon}_e\\ \dot{\omega}_E\\ \dot{a}_D\\ \dot{\varepsilon}_a\\ \dot{\omega}_D\\ \dot{a}_E\\ \dot{R}\\ \dot{V}\\ \dot{a}_R\end{pmatrix}=\begin{pmatrix}0 & 1 & 0 & \omega_r & 0 & 0 & 0 & 0 & 0\\ 0 & -2V/R & -1/R & 0 & \omega_r & 0 & 0 & 0 & 0\\ 0 & 0 & -1/\tau_D & 0 & 0 & \omega_r & 0 & 0 & 0\\ -\omega_r & 0 & 0 & 0 & 1 & 0 & 0 & 0 & 0\\ 0 & -\omega_r & 0 & 0 & -2V/R & 1/R & 0 & 0 & 0\\ 0 & 0 & -\omega_r & 0 & 0 & -1/\tau_E & 0 & 0 & 0\\ 0 & 0 & 0 & 0 & 0 & 0 & 0 & 1 & 0\\ 0 & 0 & 0 & 0 & 0 & 0 & \omega_E^2+\omega_D^2 & 0 & 1\\ 0 & 0 & 0 & 0 & 0 & 0 & 0 & 0 & -1/\tau_R\end{pmatrix}\begin{pmatrix}\varepsilon_e\\ \omega_E\\ a_D\\ \varepsilon_a\\ \omega_D\\ a_E\\ R\\ V\\ a_R\end{pmatrix}+\begin{pmatrix}-\omega_r\\ a_a/R\\ 0\\ -\omega_a\\ -a_a/R\\ 0\\ 0\\ -a_r\\ 0\end{pmatrix}+\begin{pmatrix}0 & 0 & 0\\ 0 & 0 & 0\\ 1 & 0 & 0\\ 0 & 0 & 0\\ 0 & 0 & 0\\ 0 & 1 & 0\\ 0 & 0 & 0\\ 0 & 0 & 0\\ 0 & 0 & 1\end{pmatrix}\begin{pmatrix}w_D\\ w_E\\ w_R\end{pmatrix} \quad (1)$$

Here, the first order Markov process is used to describe the target acceleration, i.e., $\dot{a}=-(1/\tau)a+w_a$. In equation (1), τ_e, τ_D, τ_R, ω_E, ω_D, and ω_R are corresponding components of τ and ω.

III. Linear Filtering and Simulation

Obviously, equation (1) is non-linear. It can be simply denoted as

$$\dot{x}(t)=f(x(t),t)+Gw(t) \quad (2)$$

It is difficult to realize in real time tracking. In order to linearize the equation of state, equation (2) was expanded into a Taylor series in the neighborhood of $\hat{x}(t)$ [6], which is the estimated value of state. By taking the first order approximation, the linearized equation is [6]

$$\dot{x}(t)=A(t)x(t)+u(t)+Gw(t) \quad (3)$$

The difference between equations (2) and (3) lies in A(t) and u(t). Respectively, A(t) and u(t) in equation (3) are [6]:

$$A(t)=\begin{pmatrix} 0 & 1 & 0 & \omega_r & 0 & 0 & 0 & 0 & 0 \\ 0 & -2\hat{V}/\hat{R} & -1/\hat{R} & 0 & \omega_r & 0 & (2\hat{V}\omega_E+\hat{a}_D-a_d)/\hat{R}^2 & -2\hat{\omega}_E/\hat{R} & 0 \\ 0 & 0 & -1/\tau_D & 0 & 0 & \omega_r & 0 & 0 & 0 \\ -\omega_r & 0 & 0 & 0 & 1 & 0 & 0 & 0 & 0 \\ 0 & -\omega_r & 0 & 0 & -2\hat{V}/\hat{R} & 1/\hat{R} & (2\hat{V}\omega_D-\hat{a}_E+a_r)/\hat{R}^2 & -2\hat{\omega}_D/\hat{R} & 0 \\ 0 & 0 & -\omega_r & 0 & 0 & -1/\tau_E & 0 & 0 & 0 \\ 0 & 0 & 0 & 0 & 0 & 0 & 0 & 1 & 0 \\ 0 & 2\hat{\omega}_E\hat{R} & 0 & 0 & 2\hat{\omega}_D\hat{R} & 0 & \hat{\omega}_E^2+\hat{\omega}_D^2 & 0 & 0 \\ 0 & 0 & 0 & 0 & 0 & 0 & 0 & 0 & 0 \end{pmatrix} \tag{4}$$

$$u(t)=[-\omega_r,\ -(\hat{a}_D-2a_d)/\hat{R},\ 0,\ -\omega_d(\hat{a}_E-2a_r)/\hat{R},\ 0,\ 0,\ -2\hat{R}(\hat{\omega}_E^2+\hat{\omega}_D^2)-a_r,\ 0]^T \tag{5}$$

It should be noticed that A(t) and u(t) are functions of $\hat{x}(t)$ and they are time dependent.

We should also consider the effect of angular blinking. A first order Markov process could be used to describe angular /51 blinking

$$\dot{s}_r(t)=-(1/\tau_r)s_r(t)+w_{,r}(t) \tag{6}$$

$$\dot{s}_d(t)=-(1/\tau_d)s_d(t)+w_{,d}(t) \tag{7}$$

Furthermore, a state expansion method was used to consider angular blinking as two state variables. The effect of angular blinking on the accuracy of the estimation could then be reduced. Thus, the state variables would be expanded to 11 dimensions, not suitable for real time estimation. Therefore, we considered the angle, range and velocity channels as statistically independent channels for separate filtering [6]:

$$
\begin{bmatrix}
\dot{\varepsilon}_r \\ \dot{\omega}_E \\ \dot{a}_D \\ \dot{s}_r \\ \dot{\varepsilon}_d \\ \dot{\omega}_D \\ \dot{a}_E \\ \dot{s}_d
\end{bmatrix}
=
\begin{bmatrix}
0 & 1 & 0 & 0 & \omega_r & 0 & 0 & 0 \\
0 & -2\hat{V}/\hat{R} & -1/\hat{R} & 0 & 0 & \omega_r & 0 & 0 \\
0 & 0 & -1/\tau_D & 0 & 0 & 0 & \omega_r & 0 \\
0 & 0 & 0 & -1/\tau_r & 0 & 0 & 0 & 0 \\
-\omega_r & 0 & 0 & 0 & 0 & 1 & 0 & 0 \\
0 & -\omega_r & 0 & 0 & 0 & -2\hat{V}/\hat{R} & 1/\hat{R} & 0 \\
0 & 0 & -\omega_r & 0 & 0 & 0 & -1/\tau_E & 0 \\
0 & 0 & 0 & 0 & 0 & 0 & 0 & -1/\tau_d
\end{bmatrix}
\begin{bmatrix}
\varepsilon_r \\ \omega_E \\ a_D \\ s_r \\ \varepsilon_d \\ \omega_D \\ a_E \\ s_d
\end{bmatrix}
+
\begin{bmatrix}
-\omega_r \\ (2a_d - \hat{a}_D)/\hat{R} \\ 0 \\ 0 \\ -\omega_d \\ (\hat{a}_E - 2a_r)/\hat{R} \\ 0 \\ 0
\end{bmatrix}
+
\begin{bmatrix}
0 & 0 & 0 & 0 \\
0 & 0 & 0 & 0 \\
1 & 0 & 0 & 0 \\
0 & 1 & 0 & 0 \\
0 & 0 & 0 & 0 \\
0 & 0 & 0 & 0 \\
0 & 0 & 1 & 0 \\
0 & 0 & 0 & 1
\end{bmatrix}
\begin{bmatrix}
w_D \\ w_{rr} \\ w_E \\ w_{rd}
\end{bmatrix}
\tag{8}
$$

$$
\begin{bmatrix} \dot{R} \\ \dot{V} \\ \dot{a}_R \end{bmatrix}
=
\begin{bmatrix}
0 & 1 & 0 \\
\hat{\omega}_E^2 + \hat{\omega}_D^2 & 0 & 1 \\
0 & 0 & -1/\tau_R
\end{bmatrix}
\begin{bmatrix} R \\ V \\ a_R \end{bmatrix}
+
\begin{bmatrix} 0 \\ -a_r \\ 0 \end{bmatrix}
+
\begin{bmatrix} 0 \\ 0 \\ 1 \end{bmatrix} w_R
\tag{9}
$$

$$
\begin{bmatrix} \dot{V} \\ \dot{a}_R \end{bmatrix}
=
\begin{bmatrix}
0 & 1 \\
0 & -1/\tau_R
\end{bmatrix}
\begin{bmatrix} V \\ a_R \end{bmatrix}
+
\begin{bmatrix} -a_r \\ 0 \end{bmatrix}
+
\begin{bmatrix} 0 \\ 1 \end{bmatrix} w_V
\tag{10}
$$

Equations (8), (9) and (10) are continuous time equations of state. The discrete equation of state and equation of measurement are as follows [7]:

$$
x(k+1) = \Phi(k+1,k)x(k) + B(k+1)u(k) + w(k) \tag{11}
$$

$$
z(k) = H(k)x(k) + v(k) \tag{12}
$$

where v(k) is the measuring noise; primarily including the thermal noise of the receiver, clutter, random measuring error, quantized error and non-linear effect of the receiver when larger tracking errors exist.

The least square of the linearization of the state vector of the dynamic system was estimated by Kalman filtering:

$$
\hat{x}(k+1|k) = \Phi(k+1,k)\hat{x}(k) + B(k+1)u(k) \tag{13}
$$

$$
\hat{x}(k+1|k+1) = \hat{x}(k+1|k) + K(k+1)[z(k+1) - H(k+1)\hat{x}(k+1|k)] \tag{14}
$$

$$
K(k+1) = P(k+1|k)H^T(k+1)[H(k+1)P(k+1|k)H^T(k+1) + R(k+1)]^{-1} \tag{15}
$$

$$
P(k+1|k) = \Phi(k+1,k)P(k)\Phi^T(k+1,k) + Q(k) \tag{16}
$$

$$P(k+1|k+1)=[I-k(k+1)H(k+1)]P(k+1|k)[I-K(k+1)H(k+1)]^{T}$$
$$+k(k+1)R(k+1)K^{T}(k+1) \qquad (17)$$

In order to investigate the performance of the tracking system after Kalman filtering, a series of simulations was carried out on a FELIX C-256 digital computer. The principle of the simulated tracking system is shown in Figure 4. During simulation, the computer created a real flight condition. It also produced engine noise, measuring noise and random noise such as angular blinking. In addition, it created observed quantities by the receiver and signal processor and formed the Kalman filter, servo control loop and antenna stabilization loop. One can refer to Reference [5] regarding the stability of airborne antennas, and Reference [7] regarding the flow chart of the computer program.

The radar carrier and the target were in relative motion in a three-dimensional space in simulation. After the target was captured, the carrier aircraft began to fly horizontally with an acceleration of $30m/s^2$ from a constant speed horizontal /52 flight. The target turned 45° to the right in front of the carrier and began to climb at an angular speed of $\sqrt{\omega_g^2+\omega_D^2}=\sqrt{150^2+150^2}=212m$ rad/s . In addition, it exercised evading maneuvers along the positive axes of the aiming axis coordinate system at an acceleration of 2G. Monte Carlo experiments showed that $1/\tau_R = 1/\tau_E = 1/\tau_D = 1/20$ during the evading maneuver. The step used in Kalman filtering calculation was T = 0.1s. When the control command was created, the weighed coefficient $\lambda = 15$.

Figure 5 shows the characteristic curves of a tracking system using Kalman filtering. EAch curve was plotted from 50 data points. Here, only the first 5 seconds were represented. Afterward, it was completely in steady state tracking. From simulation one can see that the radar tracking system has relatively higher angular and range tracking accuracies after adopting Kalman filtering. Furthermore, it is also capable of

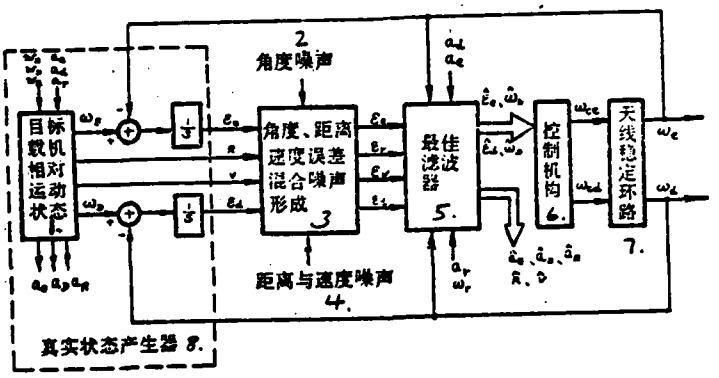

Figure 4. Principle of Tracking System Simulation.

Key: 1) Relative Motion State between Target and Carrier; 2) angular noise; 3) formation of mixed noise from errors in angles, range and velocity; 4) range and velocity noise; 5) optimal filter; 6) control mechanism; 7) antenna stabilization loop; 8) real state generator.

accurately estimating the angular velocity. It is adaptable to tracking maneuvering targets.

IV. Linear Filtering Approximation

The aforementioned linearization treatment should be permissible in engineering applications. However, the gap between this approximation and the optimum should be known. We should also understand whether there is a need to reduce this gap and the expense required to do so. To this end, we simulated non-linear filtering under the same condition as linear filtering and obtained the appropriate conclusions through comparison. Figure 6 shows the mean square root error curves for angle and angular velocity tracking [8].

It indicated that the use of non-linear filtering in angle tracking in a transient process was slightly better than Kalman filtering. The angle error was improved by 5-10% and the angular velocity error, by 10-15%. In steady state, however, there was no improvement. We also observed in simulation that the tracking

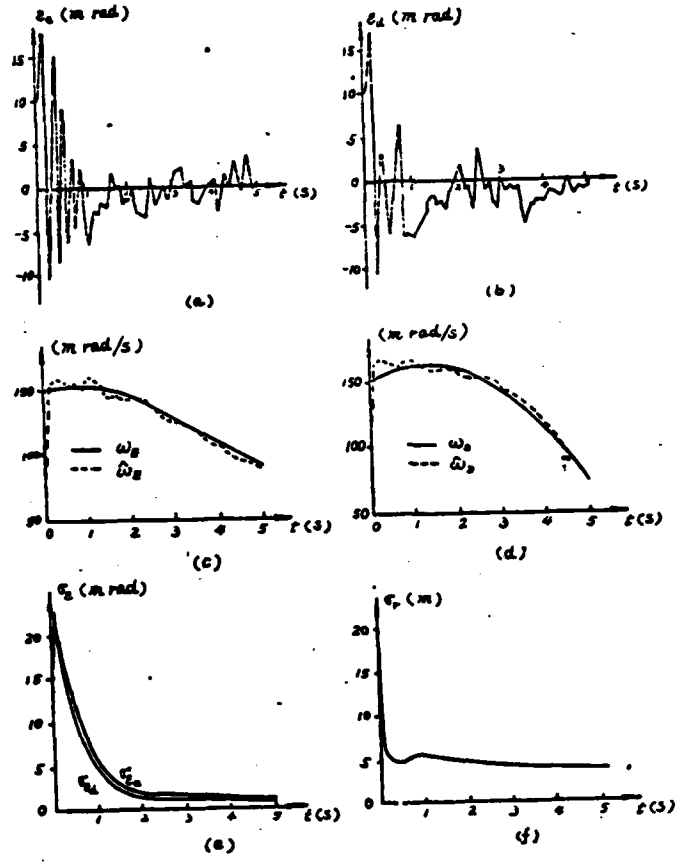

Figure 5. Performance of the Tracking System

(a) pitch angle tracking error; (b) azimuthal angle tracking error; (c) pitch angle velocity estimation; (d) azimuthal angle velocity estimation; (e) angular tracking mean square root error; (f) range tracking mean square root error.

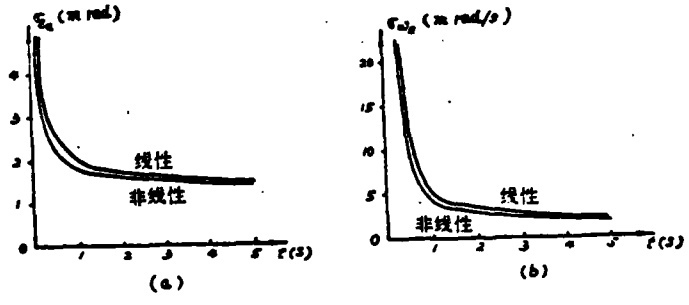

Figure 6. Mean Square Root Tracking Errors.

(a) mean square root angle error; (b) mean square root angular velocity error.

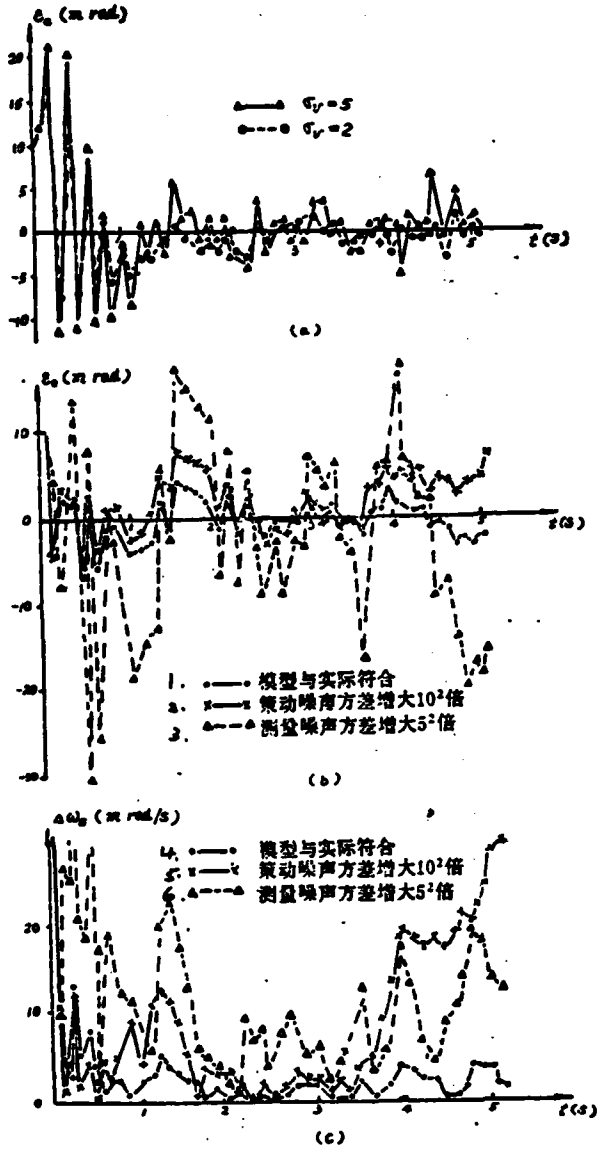

Figure 7. Effect of Noise on Tracking Accuracy

(a) Effect of Measurement Noise on ANgular Tracking (small dynamic range)
(b) Effect of Noise on Tracking Accuracy of Angles (large dynamic range)
(c) Effect of Noise on Estimation of Angular Velocity (large dynamic range)

Key: 1) model in agreement with reality; 2) square deviation of engine noise increased by 10^2; 3) square deviation of measurement noise increased by 5^2; 4) model in agreement with reality; 5) square deviation of engine noise increased by 10^2; 6) square deviation of measurement noise increased by 5^2.

performance in range and velocity was not improved by adopting non-linear filtering no matter whether it was in either transient or steady state. This further indicates that it is appropriate to use Kalman filtering. There is no need to spend several times more computations in non-linear filtering than Kalman filtering. Furthermore, because there is a characteristic "threshold" in non-linear filtering, when the signal-to-noise ratio is lower than a certain threshold, the performance may drastically deteriorate. It is not favorable in all conditions.

V. Sensitivity Simulation

The optimal condition for Kalman filtering is that the filter model coincides with the actual situation. Generally, it is not possible. The purpose of sensitivity simulation is to analyze the effect of this difference, i.e., to observe the sensitivity to changes in engine noise and measurement noise to determine the adaptability of the filter model.

The sensitivity curves of the tracking system discussed /54 in this work were obtained through simulation. Figure 7(a) shows the angle tracking error as the measurement noise varied in a small dynamic range. Figure 7(b) shows the effect of noise on angle tracking in a large dynamic range. Figure 7(c) is the effect of noise on the estimated angular velocity in a large dynamic range.

The following conclusions are obtained from the simulation:

(1) When the square deviation of the measurement noise varies in a small dynamic range, the tracking error will increase with increasing square deviation. However, the changes are not large and have no significant effect on the steady state. This system is not sensitive to noise changes in a small dynamic range.

(2) When the square deviation of measurement noise varies in a large dynamic range (by 5^2), the tracking accuracy apparently decreases. The response of the system is very sensitive.

(3) When the square deviation of engine noise varies in a large dynamic range (by 10^2), the decrease in the tracking accuracy is far less than that due to measurement noise, i.e., not as sensitive.

(4) This system is not sensitive to engine noise, demonstrating its maneuvering tracking capability. This is what we anticipate. The effect of measurement noise, however, can be corrected by measuring the signal to noise ratio.

VI. Adaptive Tracking of Maneuvering Target

When Kalman filtering was first used, maneuvering was described by a zero average white Gaussian process which is easy to treat mathematically. Obviously, the adaptivity of the filter to a maneuvering target was poor. In 1970, R. A. Singer used the zero average correlated random acceleration to describe a random maneuvering [9]. We had used this method in the simulation mentioned earlier. However, this model actually assumes that the maneuvering acceleration is a steady process. Once a filter is designed, it can only adapt to a typical maneuvering pattern. In order to overcome the shortcoming of the aforementioned method, R. L. Moose proposed a model in which a target maneuver is decomposed into the sum of white noise perturbation and finite maneuvering commands in 1973 and 1977. In 1979, R. L. Moose, et al. improved the model to a composite maneuver model. It is even closer to the real situation, i.e., the sum of the correlation process and several maneuvering instructions [10]. In this case, the adaptive filter was comprised of a Kalman filter and control command estimater. The semi-Markov process was used to describe the maneuvering control command. For the

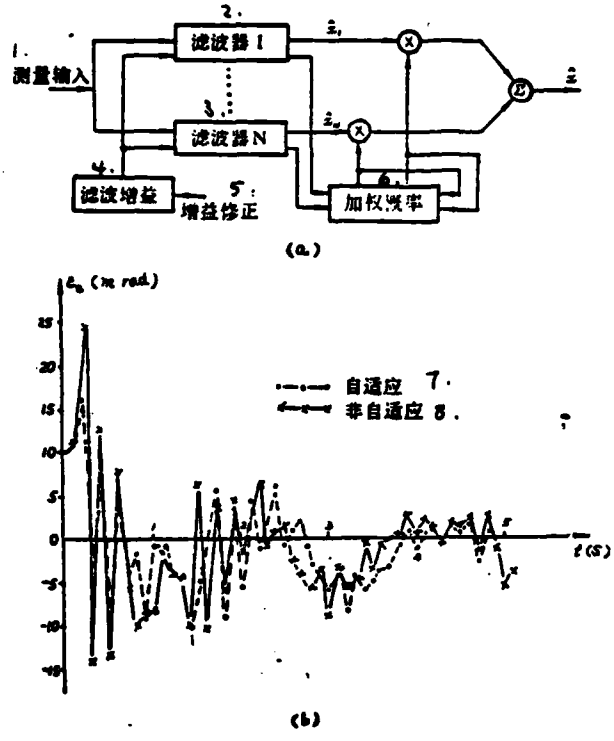

Figure 8. Adaptive Filtering

(a) Adaptive Filter; (b) Angle Tracking Error under Stepwise Command

Key: 1) input from measurement; 2) filter I; 3) filter N; 4) filter gain; 5) gain correction; 6) weighed probability; 7) adaptive; 8) non-adaptive.

first time, we applied this model to the aiming axis coordinate system of a tracking system and performed a simulation [11].

The adaptive filter system is a series of parallel filters as shown in Figure 8(a). These filters can be described as [11]:

$$\hat{x}(k|k)=\sum_{i=1}^{N}w_i(k)\hat{x}_i(k|k) \tag{18}$$

Ultimately, an adaptive filter can be built by a Kalman filter and a Bayes estimator. It can be written as [11]: /55

$$\hat{x}(k+1|k+1)=\Phi(k+1,k)\hat{x}(k|k)+\Gamma\hat{u}(k)+K(k+1)[z(k+1) -H(k+1)(\Phi(k+1,k)\hat{x}(k|k)+\Gamma(k)\hat{u}(k)] \quad (19)$$

where $\hat{u}(k)$ is the estimated value of the random control command:

$$\hat{u}(k)=\sum_{i=1}^{N}u_i w_i(k+1) \quad (20)$$

The weighted probability can be calculated based on the following formula [11]:

$$W(k+1)=c(k)A(k)\theta^T W(k) \quad (21)$$

where $W(k)=[w_1(k)\ w_2(k)\cdots w_N(k)]^T$, $c(k)$ is a normalization factor, and $A(k)$ is a time-dependent diagonal matrix whose elements can be calculated from measurement residue and input command. $\theta=[\theta_{ij}]_{N\times N}$ is the domain transformation probability matrix in the semi-Markov process. It can be calculated based on the probability of deviation from linearity. The covariance matrix of the estimated error of an adaptive filter can be corrected by the following formula [11]:

$$P_*(k|k)=P(k|k)+\left\{\sum_{i=1}^{N}w_i(k)[\hat{x}_i(k|k)-\hat{x}(k|k)][\hat{x}_i(k|k)-\hat{x}(k|k)]^T\right\} \quad (22)$$

Under the conditions of step command function, Gauss command function and exponent command function, we simulated adaptive filtering. Figure 8(b) is the adaptive and non-adaptive angle tracking error curves under a step random command. From simulations one can see that the composite maneuvering model is superior to that proposed by Singer. In a transient state, the composite maneuvering model is 25-35% better than that of Singer's. But, they are basically identical in steady state tracking.

VII. Conclusions

(1) The Kalman filtering airborne radar tracking system is superior to classical systems. It is more obvious in the presence of a maneuvering target.

(2) It is appropriate to use the aiming axis coordinate system in an airborne radar tracking system for a single target. As the coordinate system is in motion it facilitates the linearization of the model. The system has a high tracking accuracy and good adaptivity to maneuverability.

(3) The system has a high velocity tracking capability. The transient tracking characteristics of the system can be improved by choosing the composite maneuvering model.

(4) Measurement noise is one of the major factors causing tracking error. In a real system, the signal-to-noise ratio can be introduced in the calculation to determine changes in the square deviation of noise in order to correct the filtering gain.

(5) Tne weighed index is found to be $\lambda = 10 \sim 15$ in the simulation.

Mao Shiy, Li Shaohong, Zhan Shuliang, Wang Guoying, Zhang Xinghua and Zhang Zhaowu also participated in this work.

References

[1] J. B. Pearson, et al., IEEE Trans., Vol. AES-10, pp. 319-329, May 1974.
[2] U. S. P. 3,935,572, 1976.
[3] 柴田实と福坂三四郎, 电子通信学会技术研究报告, SANE 77-1.
[4] 柴田实, 福坂三四郎, 现代雷达, 1981, No.1.
[5] 张有为, 李少洪, 雷达系统分析, 国防工业出版社, 1981.
[6] 张有为, 朱谷川, 北京航空学院科研报告, BH-B656, 1981.
[7] 张有为, 朱谷川, 北京航空学院科研报告, BH-B657, 1981.
[8] 毛士艺, 王国宾, 北京航空学院科研报告, BH-B684, 1981.
[9] R. A. Singer, IEEE Trans., AES-6, No. 4, pp. 473-483, 1970.
[10] R. L. Moose, et al., IEEE Trans., AES-15, No. 3, pp. 448-456, May 1979.
[11] 朱谷川, 张有为, 北京航空学院科研报告, BH-B806, 1982.

A MODIFIED KALMAN FILTER FOR TRACKING MANEUVERING TARGETS* /57

Fang Ji-chang
(Nanjing Research Institute of Electronic Technology)

Abstract: A modified Kalman filter for tracking a maneuvering target was presented in this work based on the model of filter bank described in reference [1]. It detects a target maneuver by judging whether there is a bias in the observation residue. The maneuver acceleration command is only estimated by the damping least square method when target maneuver is detected. Furthermore, this estimate is used to correct the state-prediction and error covariance. Otherwise, it works as a single Kalman filter with its maneuver acceleration command at zero. Thus, a better compromise between the steady state filtering accuracy and fast response to maneuver is reached. Computer simulation results showed that the accuracy of the filter introduced in this work is slightly superior to that of the complicated filter bank mentioned in Reference [1]. The computation load, however, was only 1/3.6 of the latter model.

Abstract: A Modified Kalman filter,based on the model of filter bank for tracking maneuvering targets(see reference[1]), is presented in this paper.It detects the target maneuver by judging whether observation residue exhibits bias. The maneuver acceleration command is estimated by damp least squares method only when the maneuver is detected, and then the filter will correct the state-prediction and its error covariance with the estimate. Otherwise the filter works as a single Kalman filter with zero maneuver acceleration command. Thus,a better compromise between the steady filtering accuracy and rapid response to maneuver is obtained. The computer simulation results show that the filtering accuracy is somewhat better than that of Moose's complicated filter bank and the computation burden is only 1/3.6 of Moose's filter.

I. Introduction

In Reference [1], the acceleration motion of a maneuvering target was considered as a combination of a semi-Markov process [2, 3] and the Singer model [4]. A filter bank comprosed of N

*Received in July 1982, revised in February 1983.

Kalman filters was used to find N possible filtering states and their corresponding probabilities with respect to N possible maneuver acceleration commands u_i, $i \in N$. Then, their weighted average was obtained as the state filtering value at that precise moment. The mathematical model of this method is more accurate. Under the premise that the target maneuvering characteristics are known in advance, the filtering accuracy is relatively higher. However, the computation load is also heavy. It is also highly dependent upon prior knowledge. Therefore, the assumptions made for U_i may not be accurate in actual applications. In addition, all the main diagonal elements in the Markov probability transformation matrix are P and the remaining ones are $(1-P)/(N-1)$ and $(P \rightarrow 1)$. This assumption also does not completely agree with the actual situation. Therefore, the actual filtering accuracy decreases.

Most of the targets considered in this work were non-maneuvering within relatively long periods of time. They were maneuvering only small portions of time. They exhibited strong maneuvers only in even smaller fractions of time. Hence the modified Kalman filter was comprised of a single $u_i = 0$. Singer type Kalman filter with a maneuver detector and a damp type least square estimater for maneuver acceleration command. /58 Consequently, in a relatively long period of time in which u_i is indeed zero, the model coincides with the reality. The computation load, however, is lower than that for a filter bank. Furthermore, because the observation residue is used to correct the model while filtering, the deviation caused by $u_i \neq 0$ can also be better rectified.

II. Model Analysis

The equation of state and equation of measurement for the system given in Reference [1] are:

$$X_j(k+1)=\phi_j\left(\frac{k+1}{k}\right)X_j(k)+\Gamma_j\left(\frac{k+1}{k}\right)u_j(k)+\psi_j\left(\frac{k+1}{k}\right)W_j(k) \tag{1}$$

$$Z_j(k+1)=H_j(k+1)X_j(k+1)+V_j(k+1) \tag{2}$$

where j = 1, 2, 3, representing the three channels-range r, angle of elevation e and orientation b, respectively. $W_j(k)$ and $V_j(k)$ represents model noise and measurement noise, respectively. They are both zero average independent white Gauss noises. $u_j(k)$ is the maneuver acceleration command. Let us use the range channel as an example, $X_1(k+1)$、$\phi_1(k+1/k)$、$\Gamma_1(k+1/k)$、$\psi_1(k+1/k)$、$u_1(k)$、$W_1(k)$ are expressed by the following formula:

$$X_1(k+1)=\begin{bmatrix} r(k+1) \\ \dot{r}(k+1) \\ W_r'(k+1) \end{bmatrix}=\begin{bmatrix} 1 & AB \\ 0 & EF \\ 0 & 0e^{-\alpha T} \end{bmatrix}\begin{bmatrix} r(k) \\ \dot{r}(k) \\ W_r'(k) \end{bmatrix}+\begin{bmatrix} C \\ A \\ 0 \end{bmatrix}u_r(k)+\begin{bmatrix} D \\ G \\ J \end{bmatrix}W_r(k) \tag{3}$$

where $A=(1-e^{-\alpha T})/\alpha$, $B=[1+(\alpha e^{-\alpha T}-\alpha e^{-aT})/(\alpha-a)]/(\alpha a)$, $C=(\alpha T-1+e^{-\alpha T})/\alpha^2$, $D=[T+(aA-\alpha J)/(\alpha-a)]/(\alpha a)$●, $E=e^{-aT}$, $F=(e^{-aT}-E)/(a-\alpha)$, $G=(J-A)/(\alpha-a)$, $J=(1-e^{-aT})/a$, $\alpha=0.4/s$, $a=0.1/s$, } ( )*

T is the sampling time interval. $Z_1(k+1)$ is the measured value of range r(k + 1). When only the range is measured, $H_1(k+1)$ = [100].

Let $U_i = 0$. The single channel Kalman filtering equations, i.e., the expressions for state prediction, state filtering value, gain, covariance of state prediction error and covariance of state filtering error are:

$$\hat{X}\left(\frac{k+1}{k}\right)=\phi\left(\frac{k+1}{k}\right)\hat{X}\left(\frac{k}{k}\right)$$

$$\hat{X}\left(\frac{k+1}{k+1}\right)=\hat{X}\left(\frac{k+1}{k}\right)+K(k+1)\left[Z(k+1)-H(k+1)\hat{X}\left(\frac{k+1}{k}\right)\right]$$

$$K(k+1)=P\left(\frac{k+1}{k}\right)H^T(k+1)\left[H(k+1)P\left(\frac{k+1}{k}\right)H^T(k+1)+R(k+1)\right]^{-1} \tag{4}$$

$$P\left(\frac{k+1}{k}\right)=\phi\left(\frac{k+1}{k}\right)P\left(\frac{k}{k}\right)\phi^T\left(\frac{k+1}{k}\right)+\psi\left(\frac{k+1}{k}\right)Q(k)\psi^T\left(\frac{k+1}{k}\right)$$

$$P\left(\frac{k+1}{k+1}\right)=[I-K(k+1)H(k+1)]P\left(\frac{k+1}{k}\right)$$

*In Reference [1], $\overline{D=[T+(aA-\alpha T)/(\alpha-a)](\alpha a)}$, . It is believed to be mistaken.

where $Q(k) = E[W^2(k)]$, $R(k) = E[V^2(k)]$, and I is a unit matrix.

When $u_i \neq 0$, the following problems will arise if equation (4) is still used for filtering. 1. The state prediction error $\tilde{X}(k + 1/k)$ and observation residue $\tilde{Z}(k + 1/k)$ become larger. Furthermore, both are biased, because

$$\tilde{X}\left(\frac{k+1}{k}\right)=X(k+1)-\hat{X}\left(\frac{k+1}{k}\right)$$
$$=\begin{cases}\phi\left(\frac{k+1}{k}\right)\tilde{X}\left(\frac{k}{k}\right)+\psi\left(\frac{k+1}{k}\right)W(k), & u(k)=0\\ \phi\left(\frac{k+1}{k}\right)\tilde{X}\left(\frac{k}{k}\right)+\psi\left(\frac{k+1}{k}\right)W(k)+\Gamma\left(\frac{k+1}{k}\right)u(k), & u(k)\neq 0\end{cases}$$

Correspondingly,
$$E\left[\tilde{X}\left(\frac{k+1}{k}\right)\right]=\begin{cases}0, & u(k)=0\\ \Gamma\left(\frac{k+1}{k}\right)u(k), & u(k)\neq 0\end{cases} \tag{5a}$$

Then,
$$\tilde{Z}(k+1/k)=Z(k+1)-H(k+1)\hat{X}(k+1/k)=H(k+1)\tilde{X}(k+1/k)+V(k+1),$$
$$E\left[\tilde{Z}\left(\frac{k+1}{k}\right)\right]=H(k+1)E\left[\tilde{X}\left(\frac{k+1}{k}\right)\right]=\begin{cases}0, & u(k)=0\\ H(k+1)\Gamma\left(\frac{k+1}{k}\right)u(k), & u(k)\neq 0\end{cases} \tag{5b}$$

Here, $\tilde{X}(k/k) = X(k) - \hat{X}(k/k)$, which is the state filtering error. Because it is assumed that $u(k) \neq 0$ beginning at kT, therefore, $E[\tilde{X}(k/k)] = 0$ is still valid. 2. The covariance of state prediction error becomes correspondingly larger:

$$P\left(\frac{k+1}{k}\right)=E\left[\tilde{X}\left(\frac{k+1}{k}\right)\tilde{X}^{T}\left(\frac{k+1}{k}\right)\right]$$
$$=\begin{cases}\phi\left(\frac{k+1}{k}\right)P\left(\frac{k}{k}\right)\phi^{T}\left(\frac{k+1}{k}\right)+\psi\left(\frac{k+1}{k}\right)Q(k)\psi^{T}\left(\frac{k+1}{k}\right), & u(k)=0\\ \phi\left(\frac{k+1}{k}\right)P\left(\frac{k}{k}\right)\phi^{T}\left(\frac{k+1}{k}\right)+\psi\left(\frac{k+1}{k}\right)Q(k)\psi^{T}\left(\frac{k+1}{k}\right)\\ \qquad+\Gamma\left(\frac{k+1}{k}\right)Q_u(k)\Gamma^{T}\left(\frac{k+1}{k}\right), & u(k)\neq 0\end{cases} \tag{5c}$$

where $Q_u(k) = u^2(k)$. The lower equation in (5c) is an approximation. One can see that it is necessary to correct the state prediction and error covariance of a filter assuming $u(k) = u_i = 0$ when $u(k) \neq 0$. This will require us to measure and estimate u(k).

III. Maneuvering Target Detector

In Reference [1] the observation residue $\tilde{Z}(k + 1/k)$ was approximated as a Gaussian process. Its square deviation is

$$P_s(k+1/k)=E[\tilde{Z}(k+1/k)\tilde{Z}^T(k+1/k)]=\hat{H}(k+1)P(k+1/k)H^T(k+1)+R(k+1).$$

and its mean value is $E[\tilde{Z}(k+1/k)]$. In fact equation (5b) is different when $u(k) = 0$ and $\neq 0$. This is the basis for using $\tilde{Z}$ as a statistical check for u(k). As shown in Figure 1, $|\tilde{Z}|$ in the figure should be $\tilde{Z}$.

For this reason, a coincidence detector should be used. Its criterion is

$$|\tilde{Z}|>m\sqrt{P_s} \tag{6}$$

If it is satisfied consecutively n times, then it is determined that there is a maneuver command. Otherwise, it is determined that a maneuver command does not exist. Obviously, when m and n increase, the false alarm probability and spotting probability also decrease correspondingly. Otherwise, they increase accordingly. Here, $m=\sqrt{2}$, $n=2$.

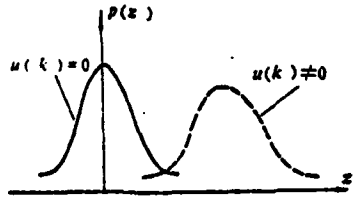

Figure 1. Probability Density Curve of Observation Residue.

IV. Damped Least Square Estimation

When u(k) ≠ 0, it is also necessary to calculate u(k) to make the correction. The relationship between u(k) and the observation residue must be derived first and then u(k) can be obtained using the damped least square method.

When u(k) ≠ 0, the state estimation based on filters where u(k) = 0 is biased (expressed with a superscript " ' "). The symbol for the unbiased estimation remains unchanged. The symbol for the corresponding observation residue also remains the same. It is not difficult to prove that the prediction of biased estimation and its observation residue are: /60

$$\hat{X}'\left(\frac{k+1}{k}\right)=\phi\left(\frac{k+1}{k}\right)\hat{X}\left(\frac{k}{k}\right)$$
$$=\phi\left(\frac{k+1}{k}\right)\left\{\left[I-K(k)H(k)\right]\hat{X}\left(\frac{k}{k-1}\right)+K(k)Z(k)\right\}$$
$$\hat{X}'\left(\frac{k+2}{k+1}\right)=\phi\left(\frac{k+2}{k+1}\right)\hat{X}'\left(\frac{k+1}{k+1}\right)$$
$$=\phi\left(\frac{k+2}{k+1}\right)\left\{\left[I-K(k+1)H(k+1)\right]\phi\left(\frac{k+1}{k}\right)\left(\left[I-K(k)\right.\right.\right.$$
$$\left.\left.\left.\cdot H(k)\right]\hat{X}\left(\frac{k}{k-1}\right)+K(k)Z(k)\right)+K(k+1)Z(k+1)\right\}$$
$$\vdots$$
$$\tilde{Z}'\left(\frac{k+1}{k}\right)=Z(k+1)-H(k+1)\hat{X}'\left(\frac{k+1}{k}\right)$$
$$\tilde{Z}'\left(\frac{k+2}{k+1}\right)=Z(k+2)-H(k+2)\hat{X}'\left(\frac{k+2}{k+1}\right) \qquad (7)$$

无偏估计及其观测残差分别为：

$$\hat{X}\left(\frac{k+1}{k}\right)=\phi\left(\frac{k+1}{k}\right)\hat{X}\left(\frac{k}{k}\right)+\Gamma\left(\frac{k+1}{k}\right)u(k)$$
$$=\phi\left(\frac{k+1}{k}\right)\left\{\left[I-K(k)H(k)\right]\hat{X}\left(\frac{k}{k-1}\right)+K(k)Z(k)\right\}$$
$$+\Gamma\left(\frac{k+1}{k}\right)u(k)$$
$$\hat{X}\left(\frac{k+2}{k+1}\right)=\phi\left(\frac{k+2}{k+1}\right)\hat{X}\left(\frac{k+1}{k+1}\right)+\Gamma\left(\frac{k+2}{k+1}\right)u(k+1)$$
$$=\phi\left(\frac{k+2}{k+1}\right)\left\{\left[I-K(k+1)H(k+1)\right]\left(\phi\left(\frac{k+1}{k}\right)\left\{\left[I-K(k)H(k)\right]\right.\right.\right.$$
$$\left.\left.\left.\hat{X}\left(\frac{k}{k-1}\right)+K(k)Z(k)\right\}+\Gamma\left(\frac{k+1}{k}\right)u(k)\right)\right.$$
$$\left.+K(k+1)Z(k+1)\right\}+\Gamma\left(\frac{k+2}{k+1}\right)u(k+1)$$

The unbiased estimation and its observation residue are:

$$\begin{aligned}\tilde{Z}\left(\frac{k+1}{k}\right)&=Z(k+1)-H(k+1)\hat{X}\left(\frac{k+1}{k}\right)\\ \tilde{Z}\left(\frac{k+2}{k+1}\right)&=Z(k+2)-H(k+2)\hat{X}\left(\frac{k+2}{k+1}\right)\end{aligned} \tag{8}$$

After subtracting equation (7) from equation (8) and moving the terms, one can get:

$$\begin{pmatrix}\tilde{Z}'\left(\frac{k+1}{k}\right)\\ \tilde{Z}'\left(\frac{k+2}{k+1}\right)\\ \vdots\end{pmatrix}=\begin{pmatrix}H(k+1)\Gamma\left(\frac{k+1}{k}\right)u(k)\\ H(k+2)\left\{\Gamma\left(\frac{k+2}{k+1}\right)u(k+1)+\phi\left(\frac{k+2}{k+1}\right)\cdot\right.\\ \left.\left[I-K(k+1)H(k+1)\right]\Gamma\left(\frac{k+1}{k}\right)u(k)\right\}\\ \vdots\end{pmatrix}+\begin{pmatrix}\tilde{Z}\left(\frac{k+1}{k}\right)\\ \tilde{Z}\left(\frac{k+2}{k+1}\right)\\ \vdots\end{pmatrix} \tag{9}$$

If the duration of u, τ, satisfies $\tau \gg lT$, then $u(k)\approx u(k+1)\approx \cdots \approx u(k+l)=u'$ [6]. Hence, equation (9) may be written in a matrix form

$$\tilde{Z}'=Cu'+\tilde{Z} \tag{10}$$

One can obtain the following by using the weighted least square estimation (Markov estimation) [5]:

$$\hat{u}=[C^{T}P_{z}^{-1}C]^{-1}C^{T}P_{z}^{-1}\tilde{Z}',\quad P_{z}=E[\tilde{Z}\tilde{Z}^{T}]. \tag{11}$$

The more data points there are in equation (9), the higher the accuracy becomes. However, the computation load and memory requirement are also higher. Furthermore, there is more delay involved. In order to synchronize real time processing and the aforementioned maneuver detection process, two points were used in a trial computation, i.e., to take $\tilde{Z}'$ and C and the 2 dimensions involved. We get

$$\hat{u}'=\frac{C_{u}P_{z}(k+2/k+1)\tilde{Z}'(k+1/k)+C_{u}P_{z}(k+1/k)\tilde{Z}'(k+2/k+1)}{C_{u}^{2}P_{z}(k+2/k+1)+C_{u}^{2}P_{z}(k+1/k)} \tag{12}$$

When equation (10) was used to estimate u', the component of became smaller as T decreased. The situation that the condition C^TC deteriorates as the least square method is used to solve the contradictory equation $CX+b\neq 0=e$ begins to appear. Or, $Cu'/\tilde{Z}$ is considerably smaller than the signal to noise ratio, affecting the accuracy of estimation. In this case, the damped least square method may be used. This method involves adding an appropriately small positive number γ to the major diagonal line of C^TC. γ is continuously iterated and varied until the satisfactory accuracy is obtained [6]. It is not suitable to use an iterative method in real time analysis. Therefore, we let $C^TP_z^{-1}C+\gamma I=\rho C^TP_z^{-1}C$, . Furthermore, the optional ρ determined experimentally ahead of time is used in equation (11). We get

$$\hat{u}=[\rho C^TP_z^{-1}C]^{-1}C^TP_z^{-1}\tilde{Z}'=\hat{u}'/\rho \tag{13}$$

ρ varies with T (as shown in Table 1). Its empirical formula is as the following:

$$\left.\begin{aligned}&\rho_e=C_{T_e}/\Gamma_u,\quad \Gamma_u=(\alpha T-1+e^{-\alpha T})/\alpha^2\\&\rho_b=1.2\rho_e,\quad \rho_r=C_{T_r}(1-e^{-\alpha T})\rho_e\end{aligned}\right\} \tag{14}$$

When u(k) ≠ 0, $\hat{u}$ is detected and estimated to perform the following correction:

$$\hat{X}\left(\frac{k+1}{k}\right)=\phi\left(\frac{k+1}{k}\right)\hat{X}\left(\frac{k}{k}\right)+\Gamma\left(\frac{k+1}{k}\right)\hat{u} \tag{15}$$

(15)

$$P\left(\frac{k+1}{k}\right)=\phi\left(\frac{k+1}{k}\right)P\left(\frac{k}{k}\right)\phi^T\left(\frac{k+1}{k}\right)+\psi\left(\frac{k+1}{k}\right)Q(k)\psi^T\left(\frac{k+1}{k}\right)$$
$$+\Gamma\left(\frac{k+1}{k}\right)\hat{u}^2\Gamma^T\left(\frac{k+1}{k}\right) \tag{16}$$

Table 1. Coefficients C_{Te} and C_{Tr} Corresponding to Sampling Interval T and ρ_r, ρ_e, ρ_b.

T \ C_{Te}, C_{Tr}	C_{Te}	C_{Tr}	ρ_r	ρ_e	ρ_b
0.5s	1.17	1.93	3.5	10	12
1s	1.27	1.92	1.9	2.9	3.5

V. Computer Simulation Results

Parameters in Reference [1] were used to generate the target trajectory data $u_i=\{\pm 14g, \pm 7g, 0\}$,. Approximately 35% of the time was used as the target. The mean square root of model error is $\sigma_x=\sigma_y=\sigma_z=15m/s^3$ The mean square root of measurement error is $\sigma_r=25m$, $\sigma_\theta=\sigma_\phi=3mrad.$ Both errors were generated by a pseudo-random number program. The measurement error was larger than that assumed in reference [1] in order to examine the performance of the filter at a lower radar measurement accuracy.

The target tracking data generated was processed by filtering methods described in the paper and Reference [1], respectively. The filtering values obtained such as r, $\dot{r}$, e, $\dot{e}$, b, $\dot{b}$ and their corresponding computer processed data and symbols were plotted as shown in Figures 2(a) ∿ (d) (only a series of examples). Table 2 also compared the filtering value of this filter and the Moose filter against the actual number with respect to T = 0.5, 0.75, 1, and 1.5s. Δ_c is the maximum filtering error of this filter and Δ_u is the maximum filtering error of the Moose filter bank. N represents the number of times the value of this filter comes closer to the actual number than that of the Moose filter out of 100 points after cancelling the number of times the two filter values approach the true value. From Table 2 one can see that in most comparisons N is a positive number. This means that there are more times this filter came closer to the actual value than those of the Moose filter. /62 Its maximum error is also slightly smaller than that of the Moose

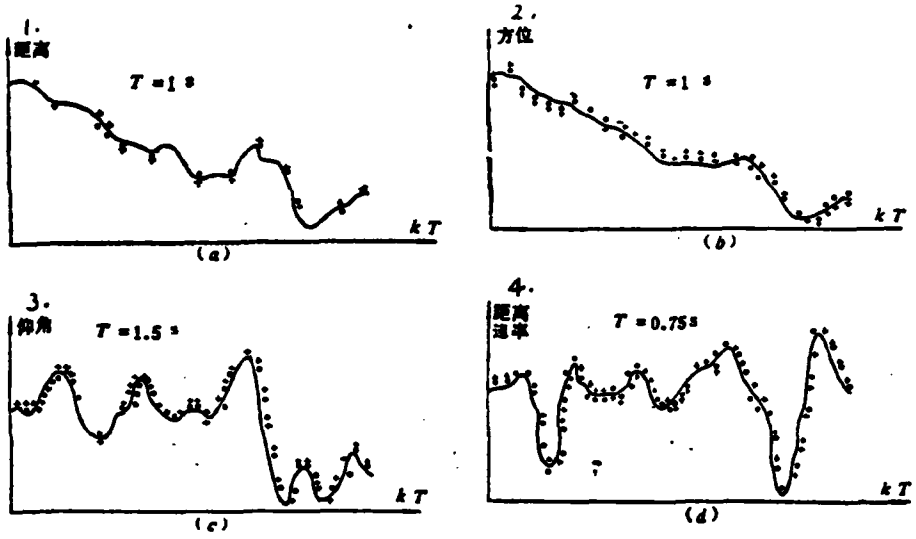

Figure 2. Results of Simulations of Two Filters.

——— represents real value
· represents filtering values of this filter
\+ represents filtering values of the Moose filter

Key: 1) range; 2) orientation; 3) angle of elevation; 4) range speed.

filter. Hence, the accuracy of this filter is slightly higher than that of the Moose filter bank.

In computer simulation, the time required for each filtering method was gathered and printed. On the same computer, the filtering of the same 100 data points requires 57.96s using the Moose filter. It only takes 16.02s using this filter. The latter is 1/3.6 of the former. Obviously, the computation load of the filter introduced in this work is significantly reduced. Therefore, there are reasons to believe that this filter is more suitable for real time processing than the Moose filter.

VI. Conclusions /63

The maneuvering target tracking filter presented in this paper uses observation residue as a check to measure and estimate the unknown model parameter - maneuver acceleration command. The

Table 2. Comparison Chart of Accuracies of Two Filters

Key: 1) compared quantity.

T(s)	比较量	N	Δ_r	Δ_θ
0.5	r	11	-62.74, 63.56m	-109.21, 121.82m
	$\dot{r}$	6		
	θ	15	- 3.34, 4.52mrad	- 3.13, 4.68mrad
	$\dot{\theta}$	12		
	b	28	- 1.64, 3.84mrad	- 3.12, 3.11mrad
	$\dot{b}$	8		
0.75	r	5	-63.21, 67.00m	- 88.88, 127.57m
	$\dot{r}$	2		
	θ	10	- 3.68, 5.73mrad	- 4.25, 5.47mrad
	$\dot{\theta}$	12		
	b	22	- 2.61, 4.92mrad	- 3.14, 4.00mrad
	$\dot{b}$	18		
1.0	r	1	-56.99 59.43m	- 73.36, 77.93m
	$\dot{r}$	-20		
	θ	- 6	- 4.19, 4.90mrad	- 4.19, 5.84mrad
	$\dot{\theta}$	9		
	b	27	- 3.91, 4.69mrad	- 3.85, 4.90mrad
	$\dot{b}$	33		
1.5	r	- 4	-52.99, 74.29m	- 55.46, 66.59m
	$\dot{r}$	-30		
	θ	-2	- 4.02, 5.66mrad	- 4.15, 5.93mrad
	$\dot{\theta}$	0		
	b	15	- 4.07, 5.08mrad	- 4.07, 5.14mrad
	$\dot{b}$	27		

function of the filter matches with the model parameters so that the computing capability is reasonably utilized. Consequently, from a certain sense, it is an "identifying and correcting while filtering model" modified Kalman filter.

This work was completed under the guidance of Senior Engineer Zhang Zhizong and comrade Qian Huisheng. The author wishes to express his gratitude.

[1] R. L. Moose, H. F. Vanlandinghan and D. H. Mccabe, IEEE Trans., Vol. AES-15, pp. 448~456, May 1979.
[2] N. H. Gholson and R. L. Moose, IEEE Trans., Vol. AES-13, pp. 310~317, May 1977.
[3] R. A. Howard, IEEE Trans., Vol. MIL-8, pp. 114~124, Apr. 1964.
[4] R. A. Singer, IEEE Trans. Vol. AES-6, pp. 473~483, July 1970.
[5] 金天鼎，最佳估计原理，上海交通大学，1979年6月。
[6] 南京大学数学系计算数学专业编，最优化方法，科学出版社，1978年。

END

FILMED

1-85

DTIC